

## Near-threshold excitation of Rydberg series by strong laser fields

G. Alber and P. Zoller

*Institute for Theoretical Physics, University of Innsbruck, 6020 Innsbruck, Austria*

(Received 15 July 1987)

We develop a theory describing laser excitation of a Rydberg series by an intense laser field. Our theory is based on the fact that the radiative coupling is restricted to a region around the atomic nucleus (the reaction zone) which is small in comparison with the extent of the excited Rydberg states. The physical processes inside the reaction zone are characterized by a few parameters which are slowly varying functions of energy across the Rydberg threshold. This finite range of the radiative coupling allows us to apply methods from quantum-defect theory and to treat the laser interaction with the Rydberg series and the adjoining electron continuum as a whole. Within this approach we derive analytical expressions for transition probabilities as a function of time in either a *dressed-state representation* which is appropriate as long as only a few Rydberg states are excited or a *multiple-scattering expansion* which is particularly suited for a description of the excitation process close to threshold. The physical picture emerging in this limit is one of a radial electronic wave packet which is generated within the reaction zone and moves in the Coulomb potential of the ionic core. Every time it returns to the inner turning point of its orbit, i.e., to the reaction zone, it is either deexcited back to the initial atomic state or is scattered by the ionic core.

### I. INTRODUCTION

Rydberg states play an important role as intermediate and final states in laser-induced ionization and excitation of atoms and molecules. The purpose of this paper is to address the problem of near-threshold excitation of Rydberg series from one of the low-lying atomic states by an intense laser field.<sup>1,2</sup> In particular the list of questions to be discussed includes the time evolution, intensity, and frequency dependence of transition probabilities close to threshold when an infinite number of both Rydberg levels and continuum states participate in the laser-induced dynamics.

Usually, laser excitation of atoms and molecules is described within models where the Schrödinger equation is solved in a finite basis of resonant atomic states in the rotating-wave approximation (in the simplest case a two-level system),<sup>3,4</sup> while the coupling to nonresonant levels is treated in perturbation theory. Diagonalizing the Hamiltonian of the atom in the laser field then leads to a set of dressed atomic states. The time dependence of the transition probabilities exhibits the familiar Rabi oscillations. Obviously, the validity of this approach is confined to an energy region far below threshold as long as the Rabi frequency which characterizes the laser-induced coupling is much smaller than the frequency separation between adjacent excited states.<sup>5,6</sup> On the other hand, transitions from bound states to the flat electron continuum are usually formulated within a pole (or Markov) approximation<sup>4</sup> which describes the (exponential) decay of a discrete state into a continuum with a rate given by Fermi's golden rule, and thus serves to define an ionization cross section. Again this approximation becomes invalid when a threshold is approached.<sup>1,2,7</sup>

In the present paper we develop a theory of near-threshold excitation with the essential feature that it treats the laser interaction with the Rydberg series as a whole, and thus includes from the very beginning both the infinite number of Rydberg states and the adjoining electron continuum. Our starting point is the observation that the coupling of the atom with the laser field can be described as a *finite-range interaction* in the sense that the laser-induced dynamics (photoabsorption) is confined to a finite reaction zone while the motion of the electron outside in the asymptotic region is determined by a pure Coulomb force. In this asymptotic regime the wave function is a linear combination of regular and irregular Coulomb functions. This allows us to apply methods from quantum-defect theory (QDT),<sup>8-10</sup> which deals with the analytical properties of these Coulomb functions. The electronic dynamics inside the reaction zone is characterized by a small set of *intensity-dependent* "quantum-defect" parameters, which as a function of energy are almost constant across the Rydberg threshold.

As far as transitions from low-lying bound states to Rydberg states are concerned this property of a finite interaction volume for the laser absorption process is obvious: the initial bound state typically has a size of a few Bohr radii which is much smaller than the extent of a Rydberg orbit so that photoabsorption to a Rydberg state occurs within a small interaction zone close to the atomic nucleus. The finite-range character of the laser interaction in optical Rydberg-free and free-free transitions has been discussed recently in detail in Ref. 11.

The property of a finite interaction volume proves essential in extracting the rapid energy dependence of the amplitudes of the Laplace-transformed time-dependent atomic wave functions due to the Rydberg resonances from a slowly varying background. In par-

ticular, this allows us to obtain closed-form analytical expressions for the time evolution of transition probabilities. This is in contrast to previous studies which either have been based on a numerical analysis<sup>2</sup> or have included the influence of the Rydberg states on the dynamics only in an approximate way.<sup>1</sup> In our case the time dependence can be obtained in a *dressed-state representation*, expressing the time evolution as a sum and integral over the spectrum of atomic dressed states which diagonalize the atomic Hamiltonian in the laser field. In this way we recover far below threshold the results of two-level theories, while for transitions far above threshold we find the expected exponential decay law for the ionization probabilities in agreement with the pole approximation. Close to threshold when a large number of Rydberg levels including the continuum contribute it is more appropriate to write the atomic amplitudes in terms of a *multiple-scattering expansion*<sup>12</sup> which expresses the transition amplitudes as an infinite sum over contributions of classical paths (Kepler orbits) of the Rydberg electron. The physical picture emerging in this limit is the one of a (radial) electronic wave packet which moves in the Coulomb potential of the ionic core and can either be excited (de-excited) by the laser from (to) the initial state or scattered (elastically or inelastically) by the ionic core in the presence of the laser field every time it returns to the inner classical turning point of its orbit, i.e., to the reaction zone. This behavior gives rise to oscillations of the initial-state probability with the period of the mean classical orbit time of the excited wave packet.

The paper is organized as follows. As an introductory example we consider in Sec. II one-photon excitation of Rydberg states neglecting possible ionization channels to higher continua. The purpose of this section is to develop the essential physical ideas of the dressed-state representation and the multiple-scattering expansion. Section III extends our study to excitation of an autoionizing Rydberg series, which allows us to study the influence of an additional decay channel. Finally in Sec. IV we take into account laser-induced transitions from the excited Rydberg states to higher electron continua.

## II. NEAR-THRESHOLD EXCITATION OF A RYDBERG SERIES—AN INTRODUCTORY EXAMPLE

In this section we discuss the dynamics of excitation of Rydberg states from an initial low-lying atomic state by an intense laser field as schematically shown in Fig. 1(a). This corresponds to the simplest possible excitation scheme. The purpose of this section is to discuss the dressed-state representation and the multiple-scattering expansion and to point out the essential physical picture emerging in the problem of near-threshold excitation.

For the wave function  $|\Psi(t)\rangle$  of the atomic electron which is excited from the initial state  $|g\rangle$  with energy  $\epsilon_g$  to Rydberg states  $|n\rangle$  with energies  $\epsilon_n$  and energy-normalized continuum states  $|\epsilon\rangle$  ( $0 \leq \epsilon < \infty$ ) we make the ansatz

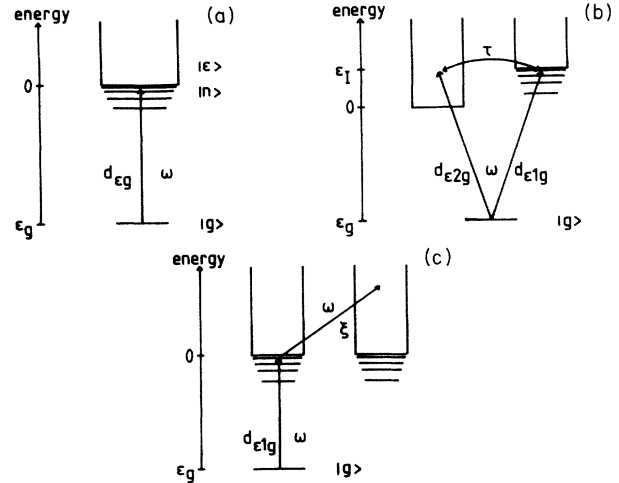


FIG. 1. Schematic representation of the excitation processes studied in Secs. II, III, and IV.

$$|\Psi(t)\rangle = |g\rangle a_g(t) + \sum_n |n\rangle a_n(t) + \int_0^\infty d\epsilon |\epsilon\rangle a_\epsilon(t) \\ \equiv |g\rangle a_g(t) + |F(t)\rangle, \quad (2.1)$$

with  $|F(t)\rangle$  characterizing the time evolution of the excited Rydberg states and the adjoining electron continuum. All formulas in the following are written in Hartree atomic units ( $e = \hbar = m = 1$ ). We assume that the electric field of the laser is turned on instantaneously at  $t = 0$  and for  $t > 0$  has the form

$$\mathbf{E}(t) = \mathcal{E} \boldsymbol{\epsilon} e^{-i\omega t} + \text{c.c.}, \quad (2.2)$$

with  $\mathcal{E}$  the amplitude,  $\omega$  the frequency, and  $\boldsymbol{\epsilon}$  the polarization of the laser light. In the rotating-wave and dipole approximations the Laplace transform of the initial-state amplitude  $a_g(z)$ , defined by

$$a_g(t) = (1/2\pi) \int_{-\infty+i0}^{+\infty+i0} dz e^{-izt} a_g(z), \quad (2.3)$$

has the solution<sup>2</sup>

$$a_g(z) = i[z - \epsilon_g - \Sigma(z + \omega)]^{-1}. \quad (2.4)$$

Here

$$\Sigma(\epsilon) = \left\langle g \left| d \mathcal{E}^* \frac{1}{\epsilon - H_A + i0} d \mathcal{E} \right| g \right\rangle \\ = \sum_n |d_{ng} \mathcal{E}|^2 / (\epsilon - \epsilon_n) \\ + \int_0^\infty d\epsilon' |d_{\epsilon'g} \mathcal{E}|^2 / (\epsilon - \epsilon' + i0) \quad (2.5)$$

is the self-energy of the initial state with  $H_A$  the atomic Hamiltonian and  $d = \mathbf{d} \cdot \boldsymbol{\epsilon}$  with the atomic dipole operator  $\mathbf{d}$ . Before proceeding to a discussion of near-threshold phenomena we find it worthwhile to review briefly the solution in the energy region far below threshold (in the two-level approximation) and far above

threshold (exponential decay of the initial-state probability due to ionization).

#### A. Far below threshold: The two-level approximation

Whenever the exciting laser field is tuned to near resonance with one of the bound states  $|n\rangle$  (i.e.,  $|\varepsilon_g + \omega - \varepsilon_n| \ll |\varepsilon_n - \varepsilon_{n\pm 1}|$ ), and the intensity is sufficiently low ( $\Omega_n = 2d_{ng}|\mathcal{E}| \ll |\varepsilon_n - \varepsilon_{n\pm 1}|$ ) so that only state  $|n\rangle$  is dominantly excited, the self-energy  $\Sigma(\varepsilon)$  as given in Eq. (2.5) may be approximated by

$$\Sigma(\varepsilon) \simeq \frac{1}{4}\Omega_n^2 / (\varepsilon - \varepsilon_n) \quad (2.6)$$

with  $\Omega_n$  the Rabi frequency. Inserting Eq. (2.6) into Eq. (2.4) we find the poles  $z_{1,2}$  of  $a_g(z)$  and the quasienergies (or dressed-state energies)  $\bar{\varepsilon}_{1,2} = z_{1,2} + \omega$  of the two-level system from the quadratic equation

$$(\bar{\varepsilon} - \bar{\varepsilon})(\bar{\varepsilon} - \varepsilon_n) - \frac{1}{4}\Omega_n^2 = 0 \quad (2.7)$$

with the mean excited energy  $\bar{\varepsilon} = \varepsilon_g + \omega$ . In particular, this equation describes the positions of the ac Stark split energy levels.

Inverting the Laplace transform we obtain

$$a_g(t) = \sum_{j=1}^2 e^{-i(\varepsilon_j - \omega)t} \frac{(\frac{1}{2}\Omega_n)^2}{(\bar{\varepsilon}_j - \bar{\varepsilon})^2 + (\frac{1}{2}\Omega_n)^2}. \quad (2.8)$$

The initial-state probability therefore exhibits the well-known Rabi oscillations with frequency  $[(\varepsilon_n - \bar{\varepsilon})^2 + \Omega_n^2]^{1/2}$ .

#### B. Far above threshold: Exponential decay

If the laser field is tuned well above the photoionization threshold, the dominant contribution to  $\Sigma(\varepsilon)$  comes from the excited continuum states near the energy-conserving value  $\varepsilon' \approx \bar{\varepsilon}$ . As the bound-free dipole matrix elements  $d_{\varepsilon g}$  are smooth functions of energy, we may approximate  $\Sigma(z + \omega)$  by its value at  $z = \varepsilon_g$  (pole approximation) (Ref. 4),

$$\Sigma(z + \omega) \simeq \delta\omega - i\gamma/2. \quad (2.9)$$

$\delta\omega$  is an approximately energy-independent quadratic Stark shift (which in the following is assumed to be absorbed in the initial-state energy  $\varepsilon_g$ ) and

$$\gamma = 2\pi |\langle \bar{\varepsilon} | d \mathcal{G} | g \rangle|^2 \quad (2.10)$$

is the ionization rate in agreement with Fermi's golden rule.<sup>3</sup> The self-energy (2.9) gives rise to a complex quasienergy at  $\bar{\varepsilon} = z + \omega = \bar{\varepsilon} - i\gamma/2$ . Inverting the Laplace transform we find

$$a_g(t) = e^{-i(\bar{\varepsilon} - \omega)t} e^{-\gamma t/2}, \quad (2.11)$$

i.e., the initial-state probability is exponentially decaying as a function of time.<sup>3</sup>

#### C. Near threshold

When the laser is tuned close to the photoionization threshold many bound and continuum states

significantly contribute to the self-energy  $\Sigma(\varepsilon)$  in Eq. (2.5). Taking the Laplace transform of  $|\Psi(t)\rangle$  we find the following system of close-coupling equations:

$$\begin{aligned} (z - \varepsilon_g)a_g(z) + \langle g | d^* \mathcal{E}^* | F(z + \omega) \rangle &= i, \\ (z + \omega - H_A) | F(z + \omega) \rangle + d \mathcal{E} | g \rangle a_g(z) &= 0. \end{aligned} \quad (2.12)$$

Systems of this type, which describe the coupling between a bound channel  $|g\rangle$  and a free channel  $|F(z + \omega)\rangle$ , have been studied in QDT.<sup>8-10</sup> In the present example the radiative coupling is of finite range due to the localization of the initial-state wave function  $|g\rangle$  to a region extending a few Bohr radii around the atomic nucleus. As is shown in Appendix A, Eq. (2.12) implies<sup>13</sup>

$$\Sigma(\varepsilon) = \begin{cases} \delta\omega - i\gamma/2 & (\varepsilon > 0) \\ \delta\omega + (\gamma/2)\cot\pi[\nu(\varepsilon) + \alpha] & (\varepsilon < 0). \end{cases} \quad (2.13)$$

Below threshold ( $\varepsilon < 0$ )  $\alpha$  is the quantum defect of the excited Rydberg series. It is due to a deviation of the ionic core potential from a pure Coulomb form. According to standard QDT assumptions this deviation is restricted to a region around the atomic nucleus (defined as the reaction zone) which is small in comparison with the extent of highly excited Rydberg states. This implies that  $\alpha$  is approximately energy independent across the Rydberg threshold. Above threshold ( $\varepsilon > 0$ ),  $\pi\alpha$  is the continuum phase shift characterizing electron-ion scattering inside the reaction zone.<sup>10</sup>  $\delta\omega$  and  $\gamma$  [see Eq. (2.10)] are a quadratic Stark-shift contribution and the ionization rate in agreement with Fermi's golden rule. As a consequence of the finite-range character of the laser interaction,  $\delta\omega$  and  $\gamma$  are (approximately) energy independent across threshold.

The rapid energy dependence of  $\Sigma(\varepsilon)$  below threshold is determined by the long-range Coulomb potential of the ionic core. This is reflected in the dependence of  $\Sigma(\varepsilon)$  on the effective quantum number  $\nu(\varepsilon) = (-2\varepsilon)^{-1/2}$ . Typically  $\Sigma(\varepsilon)$  exhibits poles at the energies of the Rydberg states  $\varepsilon_n = -\frac{1}{2}(n - \alpha)^{-2}$ .

It is not difficult to see that Eq. (2.13) reduces to the result of the two-level approximation when only a single state  $|n\rangle$  is significantly excited. Expanding the denominator of Eq. (2.13) near the resonance energy  $\varepsilon \approx \varepsilon_n$  we obtain Eq. (2.6) provided we make the identification

$$\frac{1}{4}\Omega_n^2 = \frac{\gamma}{2\pi}(n - \alpha)^{-3}. \quad (2.14)$$

Note that Eq. (2.14) implies the familiar  $(n - \alpha)^{-3/2}$  scaling of dipole matrix elements  $d_{ng}$  from the initial state  $|g\rangle$  to Rydberg states  $|n\rangle$ .<sup>8</sup> Above threshold Eq. (2.13) is identical with Eq. (2.9).

The dressed-state energies  $\bar{\varepsilon}_n = z_n + \omega$  are determined by the poles of  $a_g(z)$ . According to Eqs. (2.13) and (2.4) they are solutions of the transcendental equation

$$\bar{\varepsilon}_n = -\frac{1}{2}[n - \alpha - \mu(\bar{\varepsilon}_n)]^{-2} \quad (2.15)$$

with the intensity-dependent quantum defect

$$\mu(\varepsilon) = (-1/\pi) \arctan[(\gamma/2)(\varepsilon - \bar{\varepsilon})^{-1}] .$$

The rapid energy variation of  $\mu(\varepsilon)$  around the mean excited energy  $\bar{\varepsilon}$  reflects the fact that the laser field tends to pull the quasienergies  $\bar{\varepsilon}_n$  away from  $\bar{\varepsilon}$ . The appearance of an intensity-dependent quantum defect is not surprising. It is well known that the mixing of a bound state into a continuum leads to a resonant phase shift  $\pi\mu(\varepsilon)$ .<sup>14</sup> In the case of excitation from a low-lying atomic state such a continuum phase shift manifests itself in the appearance of laser-induced autoionizinglike resonances<sup>15</sup> whereas in the process of laser-assisted electron-ion scattering, which is described by the scatter-

ing matrix

$$\tilde{\chi}(\varepsilon) = e^{2i\pi[\alpha + \mu(\varepsilon)]} , \quad (2.16)$$

it gives rise to a "capture-escape" resonance.<sup>16</sup> On the other hand, scattering phase shifts correspond to quantum defects in the bound-state region, in agreement with Eq. (2.15).<sup>8,10</sup>

We now return to study the time evolution of the initial-state amplitude. Using Eq. (2.13) and inverting the Laplace transform by contour integration we find the initial-state amplitude in the dressed-state representation<sup>17</sup>

$$a_g(t) = \sum_n e^{-i(\bar{\varepsilon}_n - \omega)t} \frac{1}{\pi} \bar{v}_n^{-3} \frac{\gamma/2}{(\bar{\varepsilon}_n - \bar{\varepsilon})^2 + (\gamma/2)^2} \left[ 1 + \frac{2}{\gamma\pi} \bar{v}_n^{-3} \right] + \frac{i}{2\pi} e^{-i(\bar{\varepsilon} - \omega)t} \{ e^{-\gamma t/2} [E_1(-i\bar{\varepsilon}t - \gamma t/2) - 2i\pi\Theta(\bar{\varepsilon})] - e^{\gamma t/2} E_1(-i\bar{\varepsilon}t + \gamma t/2) \} . \quad (2.17)$$

$\Theta(x)$  is the unit step function which vanishes for  $x < 0$ . The form of the integration contour is given, e.g., in Ref. 1.  $E_1(x)$  is the exponential integral as defined in Ref. 18. Equation (2.17) shows that all quasienergies in an energy interval of width  $\gamma(1 + (2/\pi\gamma)\bar{v}^{-3})^{1/2}$  around the mean excited energy  $\bar{\varepsilon}$  are significantly involved in the excitation process. We can therefore distinguish between two different dynamical regimes, namely, the two-level (or weak-field) limit characterized by  $\gamma \ll \bar{v}^{-3}$  and the threshold (or intense field) limit where  $\gamma \gg \bar{v}^{-3}$ . The last case implies

$$T_{\bar{\varepsilon}} = 2\pi(-2\bar{\varepsilon})^{-3/2} \gg 2\pi/\gamma \quad (2.18)$$

with  $T_{\bar{\varepsilon}}$  the classical orbit time of an electron of energy  $\varepsilon$  in a Coulomb potential.<sup>19</sup> In the time domain Eq. (2.18) expresses the fact that the depletion time of the initial state corresponding to the "ionization rate"  $\gamma$  as induced by the intense laser field is shorter than the classical orbit time for the electron excited into the Rydberg series.

Under condition (2.18) a direct evaluation of Eq. (2.17) is inconvenient because many dressed states contribute to the sum. Instead we prefer to represent the initial-state amplitude in the form of a multiple-scattering expansion<sup>12</sup> (for a derivation see Appendix B)

$$a_g(t) = e^{-i(\bar{\varepsilon} - \omega)t} e^{-\gamma t/2} + \sum_{m=1}^{\infty} \int_{-\infty}^0 d\varepsilon e^{-i(\varepsilon - \omega)t} [i(\varepsilon - \bar{\varepsilon} + i\gamma/2)^{-1} \mathcal{D}_{\varepsilon}^{(-)}] e^{2i\pi\nu(\varepsilon)} \times [\tilde{\chi}(\varepsilon) e^{2i\pi\nu(\varepsilon)}]^{m-1} [\mathcal{D}_{\varepsilon}^{(-)} i(\varepsilon - \bar{\varepsilon} + i\gamma/2)^{-1}] \quad (2.19)$$

with the complex photoionization amplitudes

$$\mathcal{D}_{\varepsilon}^{(-)} = -ie^{i\pi\alpha} d_{\varepsilon g} \mathcal{G} \quad (2.20)$$

and the laser-assisted electron-ion scattering matrix  $\tilde{\chi}(\varepsilon)$  as given by Eq. (2.16). Since  $\gamma \gg \bar{v}^{-3}$ ,  $e^{2i\pi\nu(\varepsilon)}$  (which involves the classical action  $2\pi\nu(\varepsilon)$  along a closed Coulomb trajectory<sup>19</sup>) is a rapidly oscillating function of energy. Therefore the dominant contribution to the energy integrals with  $m = 1, 2, \dots$  comes from points of stationary phase  $\varepsilon_s(m, t)$ , defined for given  $t$  and  $m$  by

$$t = mT_{\varepsilon_s(m, t)} \quad (m = 1, 2, \dots) . \quad (2.21)$$

Performing the energy integration in Eq. (2.19) with the stationary-phase method<sup>20</sup> we find

$$a_g(t) = e^{-i(\bar{\varepsilon} - \omega)t} e^{-\gamma t/2} + \sum_{m=1}^{\infty} (2\pi / |\Phi^{(2)}|)^{1/2} e^{i\pi/4} e^{i\Phi(\varepsilon, m, t)} (\gamma/2\pi) [(\varepsilon - \bar{\varepsilon})^2 + (\gamma/2)^2]^{-1} \Big|_{\varepsilon = \varepsilon_s(m, t)} \quad (2.22)$$

with

$$\Phi(\varepsilon, m, t) = -(\varepsilon - \omega)t + 2\pi m [v(\varepsilon) + \alpha + \mu(\varepsilon)]$$

and

$$\Phi^{(2)} \equiv \left[ \frac{\partial^2 \Phi(\varepsilon, m, t)}{\partial \varepsilon^2} \right]_{m, t} = 6\pi m (-2\varepsilon)^{-5/2}.$$

For a given time  $t$ , the only terms in Eq. (2.22) which contribute are those for which  $|\varepsilon_s(m, t) - \bar{\varepsilon}| \lesssim \gamma$ . For times  $t \ll T_{\bar{\varepsilon}}$  (i.e., for times much shorter than the classical orbit time) the initial-state amplitude therefore decays exponentially with the "ionization" rate  $\gamma$  as there are no stationary phase contributions. With  $T_{\bar{\varepsilon}}$ , which we use here and in the following for simplicity, we mean more precisely the minimum classical orbit time associated with the significantly excited Rydberg states, i.e.,  $T_{\bar{\varepsilon}} \equiv T_{\max(|\bar{\varepsilon}|, \gamma)}$ .

The depletion of the initial state  $|g\rangle$  on a time scale  $t \approx 1/\gamma \ll T_{\bar{\varepsilon}}$  implies the generation of a radial electronic wave packet because the excitation process is localized not only in space but also in time.<sup>6</sup> The exponential decay law for the initial state reflects the fact that during the formation of the wave packet the electron is not affected by the outer turning point of the Coulomb potential of the ionic core, and therefore for times  $t \ll T_{\bar{\varepsilon}}$  behaves as if in a true ionization process above threshold. For times  $t \gtrsim T_{\bar{\varepsilon}}$  the dominant contribution of Eq. (2.22) stems from the term with  $m = 1$  which describes the first return of the wave packet to the inner turning point of its orbit where it can be de-excited back to the initial state  $|g\rangle$ , which leads to a recombination of the electron-ion complex. Similar arguments can be presented for times  $t \approx mT_{\bar{\varepsilon}}$  ( $m = 2, 3, \dots$ ), so that the initial state will show population pulsations with the period of the classical orbit time. Equation (2.22) further shows that the  $m$ th contribution contains not only information about the initial excitation and final recombination but also about the intermediate  $(m - 1)$  laser-assisted electron-ion scattering events which occur whenever the excited electron approaches the core and are characterized by  $\tilde{\chi}(\varepsilon)$  of Eq. (2.16). With increasing time the wave packet will spread, which manifests itself in a broadening of the stimulated recombination peaks. The number of  $m$  terms  $\Delta m$  contributing at a particular time  $t$  to the initial-state amplitude can be estimated from Eq. (2.21) by

$$\Delta m \approx \gamma \left[ \frac{\partial m(\varepsilon, t)}{\partial \varepsilon} \right]_{t, \varepsilon = \bar{\varepsilon}} = 3[t/T_{\bar{\varepsilon}}\gamma / (-2\bar{\varepsilon})]. \quad (2.23)$$

If  $\Delta m \ll 1$  contributions due to successive returns of the excited electron to the ionic core are well separated in time. For sufficiently long times eventually  $\Delta m \gtrsim 1$  and they start to overlap. This reflects the fact that at these times the generated radial wave packet has already spread out over the whole Rydberg orbit. For these long times we can define a "mean" initial state probability by

$$\begin{aligned} \langle |a_g(t)|^2 \rangle &= \sum_{m=1}^{\infty} (2\pi / |\Phi^{(2)}|) \\ &\times \left[ \frac{1}{\pi} \frac{\gamma/2}{(\varepsilon - \bar{\varepsilon})^2 + (\gamma/2)^2} \right]^2 \Big|_{\varepsilon = \varepsilon_s(m, t)}. \end{aligned} \quad (2.24)$$

Thereby we have neglected all quantum-mechanical interferences between probability amplitudes due to successive returns of the excited electron which give rise to rapid oscillations of the initial-state probability around this mean value. Replacing the sum by an integral we find in the long-time limit  $t \gg \gamma^{-3/2}$

$$\begin{aligned} \langle |a_g(t)|^2 \rangle &= \langle |a_g(\infty)|^2 \rangle - \frac{1}{5}(t/2\pi)^{-5/3} \left[ \frac{1}{\pi} \frac{\gamma/2}{\bar{\varepsilon}^2 + (\gamma/2)^2} \right]^2. \end{aligned} \quad (2.25)$$

The "mean" population trapped in the initial state is given by

$$\begin{aligned} \langle |a_g(\infty)|^2 \rangle &= \frac{\gamma^{1/2}}{\pi} \left[ \frac{3}{2} [(2\bar{\varepsilon}/\gamma)^2 + 1]^{1/4} \cos \left[ \frac{\phi - \pi}{2} \right] \right. \\ &\quad \left. + [(2\bar{\varepsilon}/\gamma)^2 + 1]^{3/4} \sin \left[ \frac{\phi - \pi}{2/3} \right] \right] \end{aligned} \quad (2.26)$$

with

$$\tan \phi = -\frac{\gamma/2}{\bar{\varepsilon}} \quad (0 \leq \phi < 2\pi).$$

Equation (2.25) shows that in the long-time limit  $\langle |a_g(t)|^2 \rangle$  is monotonically increasing and approaches its asymptotic value according to a power law involving  $t^{-5/3}$ , which is a universal feature of threshold excitation of a Rydberg series. A result similar to Eqs. (2.25) and (2.26) has been obtained for the special case  $|\bar{\varepsilon}| \ll \gamma$  in Ref. 2 by a numerical analysis.

In Fig. 2 we have plotted the initial-state probability as a function of time for different mean excited energies  $\bar{\varepsilon}$  and a fixed value of  $\gamma$  ( $\alpha = 0$ ). Figure 2(a) represents a case where only a few quasienergies contribute to Eq. (2.17) giving rise to slightly modified Rabi oscillations. As soon as the mean ionization time  $1/\gamma$  becomes comparable to or smaller than the mean classical orbit time  $T_{\bar{\varepsilon}}$  the time dependence of the ground-state probability drastically changes [Figs. 2(b)–2(d)]. In Fig. 2(c) many Rydberg states are excited and the initial-state probability reflects the dynamics of the generated radial electronic wave packet. Whenever it returns to the inner turning point of its orbit it is de-excited back to the initial state, which corresponds to a stimulated recombination of the disintegrated electron-ion complex. The broadening of the recombination peaks with increasing time reflects the spreading of the excited wave packet. If we excite so close to threshold that  $|\bar{\varepsilon}| \lesssim \gamma$ , many  $m$  terms

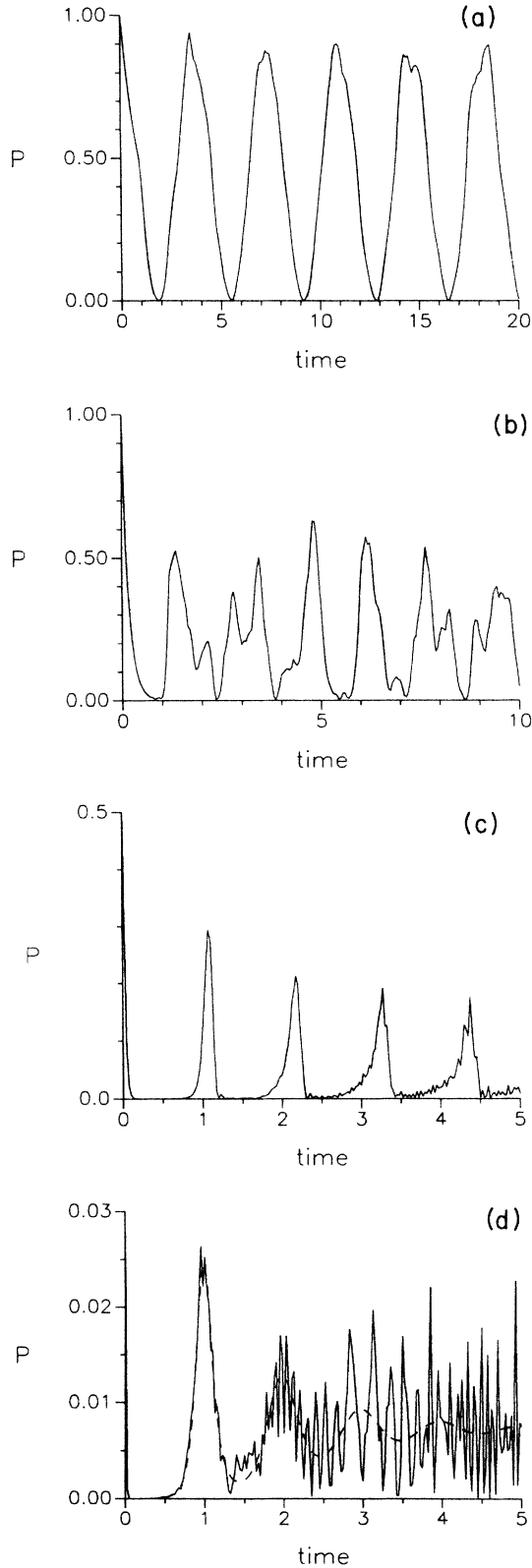


FIG. 2. Initial-state probability as a function of time (in units of  $T_{\bar{e}}$ ) in the case of excitation of a Rydberg series of bound states for  $\gamma=10^{-6}$  and  $\bar{\epsilon}=-2\times 10^{-4}$  (a),  $\bar{\epsilon}=-0.5\times 10^{-4}$  (b),  $\bar{\epsilon}=-1.25\times 10^{-5}$  (c), and  $\bar{\epsilon}=-4\times 10^{-6}$  (d). The dashed curve in (d) shows the mean initial-state probability.

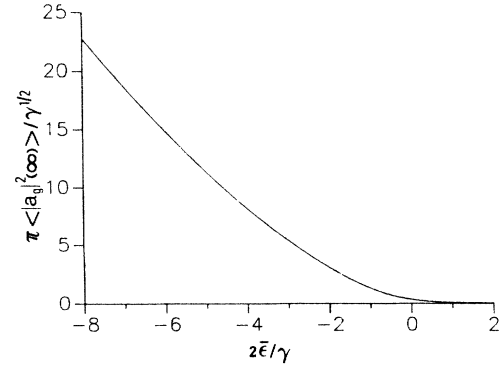


FIG. 3. Mean trapped initial-state population as a function of  $2\bar{\epsilon}/\gamma$  in units of  $\gamma^{1/2}/\pi$ .

in Eq. (2.22) contribute for times  $t \gtrsim T_{\bar{e}}$ , which gives rise to a complicated time dependence because of quantum-mechanical interferences between contributions due to successive returns of the excited electron [Fig. 2(d)]. Figures 2(a)–2(c) have been obtained with the help of Eq. (2.17). For the evaluation of the initial-state probability in Fig. 2(d) we have used Eq. (2.22). The corresponding result based on Eq. (2.17) is not shown as it is indistinguishable from the curve shown in Fig. 2(d). The dashed line in Fig. 2(d) shows the mean initial-state probability as defined by Eq. (2.24) where any quantum-mechanical interference effects are neglected. Typically we observe a damping of the oscillatory behavior of  $\langle |a_g(t)|^2 \rangle$  after a few orbit times and the approach of a steady-state value [given by Eq. (2.26)] in the long-time limit.

The mean initial-state probability  $\langle |a_g(\infty)|^2 \rangle$  measures the degree of recombination of the disintegrated electron-ion complex which is formed after a time of the order of  $1/\gamma$ . This quantity is plotted in Fig. 3 as a function of  $2\bar{\epsilon}/\gamma$  in units of  $\gamma^{1/2}/\pi$ . As more and more continuum states are excited the radial electronic wave packet tends to leave the ionic core without returning back to the core where it can recombine. This manifests itself in the monotonical decrease of  $\langle |a_g(\infty)|^2 \rangle$  as we approach and cross the ionization threshold.

### III. EXCITATION OF AN AUTOIONIZING RYDBERG SERIES

In this section we study the influence of an additional decay channel of the excited Rydberg states due to autoionization on the dynamics of the excitation process close to threshold.

Generalizing Eq. (2.1) we make the ansatz

$$\Psi(\mathbf{x}, t) = a_g(t)\Phi_g(\Omega, \rho) + \sum_{j=1}^2 \Phi_j(\Omega)F^{(j)}(\rho, t)/\rho \quad (3.1)$$

for the wave function describing the excitation process shown in Fig. 1(b).  $\Phi_j(\Omega)$  is the wave function of the ionic core of channel  $j$ .  $\Omega$  denotes the core coordinates and the angular momentum and spin of the excited electron in a particular coupling scheme.  $\Phi_g(\Omega, \rho)$  is the wave function of the initial atomic state. In the dipole-

and rotating-wave approximation the Laplace transforms of the radial part of the electronic wave function  $F^{(j)}(\rho, z)$  and of the initial-state amplitude  $a_g(z)$  are determined by

$$(z - \varepsilon_g) a_g(z) + \sum_{j=1}^2 \int_0^\infty d\rho D_j^*(\rho) F^{(j)}(\rho, z + \omega) = i, \quad (3.2)$$

$$\begin{pmatrix} z + \omega - \varepsilon_I - h_A^{(1)} & V_{12}(\rho) \\ V_{12}(\rho) & z + \omega - h_A^{(2)} \end{pmatrix} \times \begin{pmatrix} F^{(1)}(\rho, z + \omega) \\ F^{(2)}(\rho, z + \omega) \end{pmatrix} + a_g(z) \begin{pmatrix} D_1(\rho) \\ D_2(\rho) \end{pmatrix} = 0. \quad (3.3)$$

$h_A^{(j)}$  is the radial part of the atomic Hamiltonian of channel  $j$  and the thresholds of channels 1 and 2 are located at  $z + \omega = \varepsilon_I$  and  $z + \omega = 0$ . The laser-induced coupling is characterized by the radial-dependent dipole matrix elements  $D_j(\rho) = \rho \int d\Omega \Phi_j^*(\Omega) d \mathcal{E} \Phi_g(\Omega, \rho)$   $j=1,2$ . The homogeneous part of Eq. (3.3) describes the configuration interaction between both excited channels.  $V_{12}(\rho)$  is the electrostatic potential responsible for this mixing which leads to autoionization of channel 1. According to standard QDT treatments of interchannel coupling<sup>8-10</sup> we assume that  $V_{12}(\rho) \simeq 0$  for  $\rho \gtrsim \rho_c$ , with the core radius  $\rho_c$  of the order of a few Bohr radii. In addition we have  $D_j(\rho) \simeq 0$  for  $\rho \gtrsim \rho_c$ , which reflects the finite range of the radiative coupling.

Following Seaton<sup>8</sup> we characterize the configuration mixing between both excited channels within the reaction zone ( $\rho \lesssim \rho_c$ ) by the  $2 \times 2$  scattering matrix

$$\begin{aligned} \chi_{11} &= \frac{(1-\tau)}{(1+\tau)} e^{2i\pi\alpha}, \\ \chi_{22} &= \frac{(1-\tau)}{(1+\tau)} e^{2i\pi\delta}, \\ \chi_{12} &= \chi_{21} = \frac{2i\sqrt{\tau}}{(1+\tau)} e^{i\pi(\alpha+\delta)}. \end{aligned} \quad (3.4)$$

$\pi\alpha$  and  $\pi\delta$  may be identified with the unperturbed continuum phase shifts (quantum defects) of channels 1 and 2.  $\tau$  is a channel-mixing parameter.

The photoionization dipole matrix element between the initial state and channel  $k$ ,

$$\mathcal{D}_{\varepsilon k}^{(-)} = \sum_{j=1}^2 \int_0^\infty d\rho [\mathcal{F}_k^{(j)(-)}(\rho, \varepsilon)]^* D_j(\rho) \quad (k=1,2), \quad (3.5)$$

is determined by the energy-normalized regular solution  $\mathcal{F}_k^{(j)(-)}(\rho, \varepsilon)$  of the homogeneous part of Eq. (3.3) with outgoing-wave boundary conditions in channel  $k$ . These quantities are related to the corresponding real (standing-wave) dipole matrix elements  $d_{\varepsilon k g}$  ( $k=1,2$ ) by<sup>8</sup>

$$\begin{aligned} \mathcal{D}_{\varepsilon 1}^{(-)} &= -ie^{i\pi\alpha} (d_{\varepsilon 1g} + i\sqrt{\tau} d_{\varepsilon 2g}) \mathcal{E} / (1+\tau), \\ \mathcal{D}_{\varepsilon 2}^{(-)} &= -ie^{i\pi\delta} (d_{\varepsilon 2g} + i\sqrt{\tau} d_{\varepsilon 1g}) \mathcal{E} / (1+\tau). \end{aligned} \quad (3.6)$$

For the following it is convenient to introduce the Fano  $q$  parameter

$$q = -d_{\varepsilon 1g} / (\sqrt{\tau} d_{\varepsilon 2g}), \quad (3.7)$$

which measures the relative strengths of the direct radiative transition from the initial state to channel 1 and the indirect one via channel 2, which also involves configuration mixing.

In summary, the dynamics of the excited electron inside the reaction zone is characterized by the  $2 \times 2$  matrix  $\chi$  and the photoionization-dipole matrix elements  $\mathcal{D}_{\varepsilon 1}^{(-)}$  and  $\mathcal{D}_{\varepsilon 2}^{(-)}$ , which are approximately energy independent across the photoionization threshold.

The time evolution of the initial-state probability is determined by the self-energy  $\Sigma(\varepsilon)$  as defined in Eq. (2.5). Using well-known analytical properties of Coulomb functions we show in Appendix A that this self-energy can be written in the form

$$\Sigma(\varepsilon) = \begin{cases} \delta\omega - i\Gamma/2 & (\varepsilon > \varepsilon_I) \\ \tilde{\delta}\omega - i\gamma_2/2 + (\gamma_2/2)(q-i)^2/[x(\varepsilon)+i] & (\varepsilon < \varepsilon_I) \end{cases} \quad (3.8)$$

with the total ionization rate  $\Gamma = 2\pi \sum_{k=1}^2 |\mathcal{D}_{\varepsilon k}^{(-)}|^2$  and the quadratic Stark-shift contribution  $\delta\omega$ , which below threshold ( $\varepsilon < \varepsilon_I$ ) is modified to  $\tilde{\delta}\omega = \delta\omega + \gamma_2 \tau q / (1+\tau)$  due to the presence of the autoionizing resonances ( $\delta\omega$  and  $\tilde{\delta}\omega$  are in the following absorbed in the initial-state energy  $\varepsilon_g$ ). Furthermore, we have defined  $x(\varepsilon) = \tan\pi[\nu(\varepsilon) + \alpha]/\tau$  with the effective quantum number  $\nu(\varepsilon) = [2(\varepsilon_I - \varepsilon)]^{-1/2}$  and the ionization rate  $\gamma_2 = 2\pi d_{\varepsilon 2g}^2 \mathcal{E}^2$ . In the limit  $\tau \rightarrow 0$  and  $\mathcal{D}_{\varepsilon 2}^{(-)} \rightarrow 0$  Eq. (3.8) reduces to the self-energy  $\Sigma(\varepsilon)$  given in Eq. (2.13).

#### A. Initial-state probability

The initial-state amplitude  $a_g(t)$  is obtained from Eq. (2.4) by using Eq. (3.8) for the self-energy and inverting the Laplace transform by contour integration (compare with Sec. II). The quasienergies  $\tilde{\varepsilon}_n = z_n + \omega < \varepsilon_I$  are determined by the condition<sup>8</sup>

$$\tilde{\chi}_{11}(\tilde{\varepsilon}_n) - e^{-2i\pi\nu(\tilde{\varepsilon}_n)} = 0 \quad (\tilde{\varepsilon}_n < \varepsilon_I), \quad (3.9)$$

with

$$\tilde{\chi}_{11}(\varepsilon) = \chi_{11} + 2i\pi \mathcal{D}_{\varepsilon 1}^{(-)} (\varepsilon - \bar{\varepsilon} + i\Gamma/2)^{-1} \mathcal{D}_{\varepsilon 1}^{(-)} \quad (3.10)$$

characterizing the elastic electron-ion scattering process in channel 1 under the influence of the laser field inside the reaction zone. The laser field thereby induces radiative transitions to the initial atomic state  $|g\rangle$ . Equation (3.9) determines the quasienergies of an autoionizing Rydberg series which is coupled to a single interloper. This problem has been studied in the context of complex resonances.<sup>21</sup>

Before we proceed to the general case of threshold excitation it is instructive to consider the excitation of an isolated autoionizing resonance positioned at  $\varepsilon_n = -\frac{1}{2}(n-\alpha)^{-2}$  well below threshold so that  $\tau \ll 1$

and  $\Gamma \ll \nu_n^{-3}$ . Defining the autoionization rate  $\Gamma_n = (2\tau/\pi)(n-\alpha)^{-3}$  and the Rabi frequency  $\Omega_n = (\gamma_2 \Gamma_n q^2)^{1/2}$  we find for the resolvent of the initial state

$$a_g(z) = i[z + \omega - \bar{\varepsilon} + i\gamma_2/2 - \frac{1}{4}\Omega_n^2(1-i/q)^2/(z + \omega - \varepsilon_n + i\Gamma_n/2)]^{-1}. \quad (3.11)$$

This relation is well known and the associated time dependence of the initial-state probability has been studied in the context of strong-field excitation of isolated autoionizing resonances.<sup>22</sup>

If  $\Gamma \gg \bar{\nu}^{-3}$  the number of excited resonances is large and the usual contour-integration method becomes inconvenient for determining  $a_g(t)$ . In this case we use the multiple scattering expansion of the initial-state amplitude,

$$a_g(t) = e^{-i(\bar{\varepsilon}-\omega)t} e^{-\Gamma t/2} + \sum_{m=1}^{\infty} \int_{-\infty}^{\varepsilon_I} d\varepsilon e^{-i(\varepsilon-\omega)t} [i(\varepsilon - \bar{\varepsilon} + i\Gamma/2)^{-1} \mathcal{D}_{\varepsilon 1}^{(-)}] \times e^{2i\pi\nu(\varepsilon)} [\tilde{\chi}_{11}(\varepsilon) e^{2i\pi\nu(\varepsilon)}]^{m-1} [\mathcal{D}_{\varepsilon 1}^{(-)} i(\varepsilon - \bar{\varepsilon} + i\Gamma/2)^{-1}], \quad (3.12)$$

which is derived in Appendix B.

As many autoionizing resonances are excited,  $e^{2i\pi\nu(\varepsilon)}$  is a rapidly oscillating function of energy and Eq. (3.12) can be evaluated by stationary-phase methods. The energy integrals get their dominant contributions for a given  $m$  and  $t$  from energies  $\varepsilon_s(m, t)$  with  $t = mT_{\varepsilon_s(m, t)}$ . The straightforward stationary-phase evaluation of Eq. (3.12) yields

$$a_g(t) = e^{-i(\varepsilon-\omega)t} e^{-\Gamma t/2} + \sum_{m=1}^{\infty} [2\pi/|\Phi^{(2)}|]^{1/2} e^{i\pi/4} e^{-i(\varepsilon-\omega)t} [i(\varepsilon - \bar{\varepsilon} + i\Gamma/2)^{-1} \mathcal{D}_{\varepsilon 1}^{(-)}] e^{2i\pi\nu(\varepsilon)} \times [\tilde{\chi}_{11}(\varepsilon) e^{2i\pi\nu(\varepsilon)}]^{m-1} [\mathcal{D}_{\varepsilon 1}^{(-)} i(\varepsilon - \bar{\varepsilon} + i\Gamma/2)^{-1}] |_{\varepsilon=\varepsilon_s(m, t)}. \quad (3.13)$$

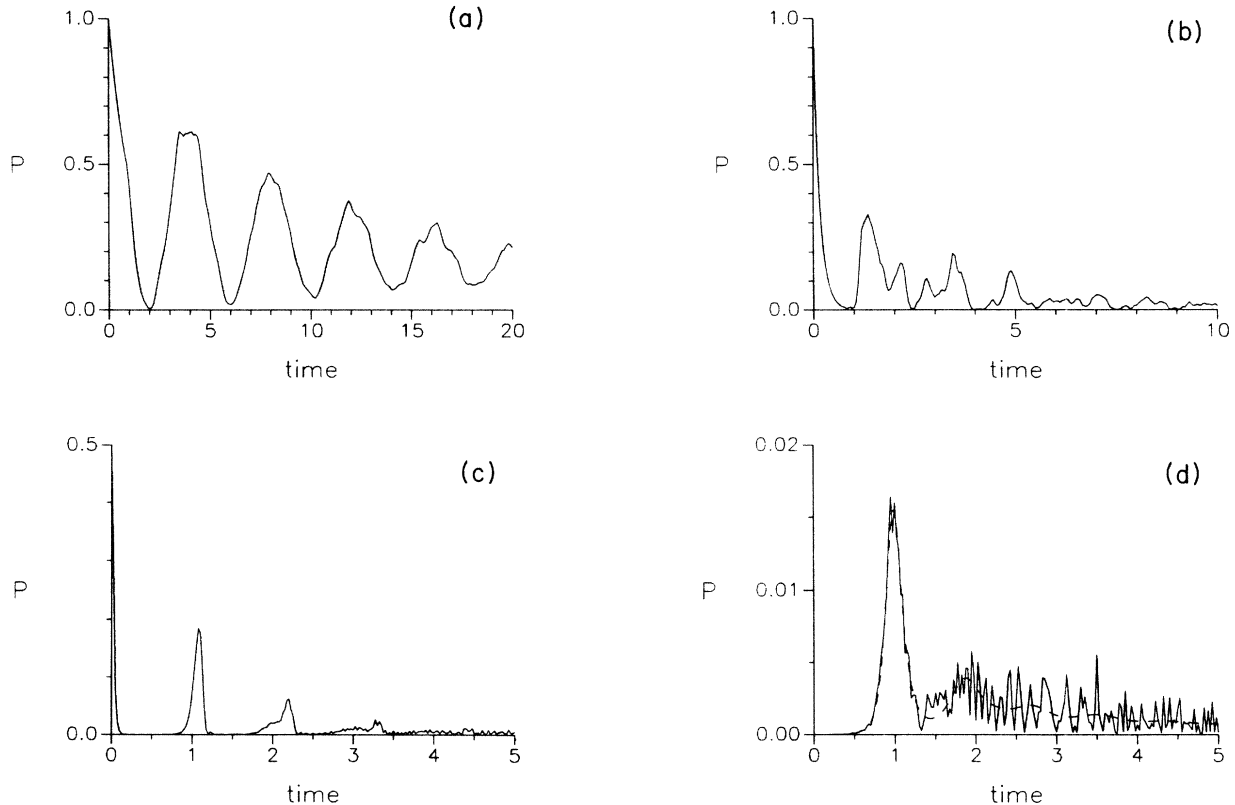


FIG. 4. Initial-state probability as a function of time (in units of  $T_{\bar{\varepsilon}}$ ) in the case of excitation of a Rydberg series of autoionizing states for  $\Gamma = 10^{-6}$ ,  $\tau = 10^{-2}$ ,  $q = 20$ , and  $\bar{\varepsilon} - \varepsilon_I = -2 \times 10^{-4}$  (a),  $\bar{\varepsilon} - \varepsilon_I = -0.5 \times 10^{-4}$  (b),  $\bar{\varepsilon} - \varepsilon_I = -1.25 \times 10^{-5}$  (c), and  $\bar{\varepsilon} - \varepsilon_I = -4 \times 10^{-6}$  (d). The dashed curve in (d) shows the mean initial-state probability.

For times much smaller than  $T_{\bar{\epsilon}}$   $a_g(t)$  is exponentially decaying on a time scale of the order of  $1/\Gamma$  and a radial Rydberg wave packet is generated. As soon as  $t \gtrsim T_{\bar{\epsilon}} \gg 1/\Gamma$  the initial-state amplitude is dominantly determined by contributions which reflect the bounded motion of the excited electron in the Coulomb potential of the ionic core.

In Fig. 4 we show the initial-state probability as a function of time for different values of the mean excited energy  $\bar{\epsilon}$  and fixed values of  $q$ ,  $\alpha$ ,  $\tau$ ,  $\Gamma$  ( $\alpha=0$ ). Figure 4(a) represents excitation of only a few autoionizing resonances. Typically we observe slightly modified Rabi oscillations which decrease in amplitude due to the fact that the initial state can decay into the open channel 2 with a rate  $\Gamma_2 = 2\pi |\mathcal{D}_{\bar{\epsilon}2}^{(-)}|^2$ . This is reflected also in Figs. 4(b)–4(d) which show the change in the time dependence of the initial-state probability as we increase the laser frequency. In the case of Fig. 4(c) many Rydberg states are excited and a radial electronic wave packet is generated. Each time it returns to the core it can

be deexcited back to the initial state. In Fig. 4(d) for  $t \gtrsim T_{\bar{\epsilon}}$  contributions due to successive returns of the excited electron to the core overlap in time. As in Sec. II Figs. 4(a)–4(c) have been obtained by summation over the contributions of all dressed states whereas Fig. 4(d) has been evaluated by using Eq. (3.13).

### B. Ionization probability

We now study the ionization probability of channel 1, i.e., the probability of finding the excited electron in this channel within the energy range  $(\epsilon_I, \infty)$ . In Appendix A we show that the Laplace-transformed excitation amplitude of channel 1 is given by [see Eq. (A12)]

$$a_{\epsilon}^{(1)}(z + \omega) = -\mathcal{D}_{\epsilon 1}^{(-)} a_g(z) / (z + \omega - \epsilon). \quad (3.14)$$

As in Eq. (3.12) we can represent the time evolution of the excitation amplitude by a multiple scattering expansion

$$\begin{aligned} a_{\epsilon}^{(1)}(t) = & [-\mathcal{D}_{\bar{\epsilon}1}^{(-)} / (\epsilon - \bar{\epsilon} + i\Gamma/2)] [e^{-i\epsilon t} - e^{-i\bar{\epsilon}t} e^{-\Gamma t/2}] \\ & + \sum_{m=1}^{\infty} \int_{-\infty}^{\epsilon_I} d\epsilon' e^{-i\epsilon' t} [(-)\mathcal{D}_{\epsilon 1}^{(-)} / (\epsilon' - \epsilon)] [i(\epsilon' - \bar{\epsilon} + i\Gamma/2)^{-1} \mathcal{D}_{\bar{\epsilon}1}^{(-)}] \\ & \times e^{2i\pi\nu(\epsilon')} [\tilde{\chi}_{11}(\epsilon') e^{2i\pi\nu(\epsilon')}]^{m-1} \mathcal{D}_{\bar{\epsilon}1}^{(-)} [i(\epsilon' - \bar{\epsilon} + i\Gamma/2)^{-1}]. \end{aligned} \quad (3.15)$$

In the case of excitation close to threshold the dominant contribution to the energy integrals for fixed values of  $t$  and  $m$  again comes from points of stationary phase  $\epsilon_s(m, t)$  with  $t = mT_{\epsilon_s(m, t)}$  and a stationary-phase evaluation of Eq. (3.15) is straightforward.

The first term of Eq. (3.15) describes the direct excitation which does not involve any return of the excited electronic wave packet to the ionic core and gives the dominant contribution for times  $t \ll T_{\bar{\epsilon}}$ . In this case we find for the ionization probability into channel 1

$$\begin{aligned} P_1(t) = \int_{\epsilon_I}^{\infty} d\epsilon |a_{\epsilon}^{(1)}(t)|^2 = & 2\pi |\mathcal{D}_{\bar{\epsilon}1}^{(-)}|^2 / \Gamma (1 + e^{-\Gamma t}) \left\{ \frac{1}{2} + (1/\pi) \arctan[2(\bar{\epsilon} - \epsilon_I) / \Gamma] \right\} \\ & + (2 |\mathcal{D}_{\bar{\epsilon}1}^{(-)}|^2 / \Gamma) \text{Im}(E_1 [i(\bar{\epsilon} - \epsilon_I)t + \Gamma t/2] + e^{-\Gamma t} \{ E_1 [-i(\bar{\epsilon} - \epsilon_I)t - \Gamma t/2] - 2i\pi\Theta(\bar{\epsilon} - \epsilon_I) \}). \end{aligned} \quad (3.16)$$

Well above the second ionization threshold this reduces to the expected expression

$$P_1(t) = (2\pi |\mathcal{D}_{\bar{\epsilon}1}^{(-)}|^2 / \Gamma) (1 - e^{-\Gamma t}) \quad (\bar{\epsilon} - \epsilon_I \gg \Gamma). \quad (3.17)$$

At threshold we find

$$P_1(t) = (2\pi |\mathcal{D}_{\bar{\epsilon}1}^{(-)}|^2 / \Gamma) (1 - e^{-\Gamma t}) / 2 \quad (|\bar{\epsilon} - \epsilon_I| \ll \Gamma), \quad (3.18)$$

reflecting the fact that with a probability of  $\frac{1}{2}$  the autoionizing Rydberg states close to threshold are excited; they decay into channel 2 and are therefore lost for the ionization signal  $P_1(t)$ . If the initial state is completely depleted we obtain from Eq. (3.16)

$$\begin{aligned} P_1(t) = & (2\pi |\mathcal{D}_{\bar{\epsilon}1}^{(-)}|^2 / \Gamma) \\ & \times \left\{ \frac{1}{2} + (1/\pi) \arctan[2(\bar{\epsilon} - \epsilon_I) / \Gamma] \right\} \quad (1/\Gamma \ll t \ll T_{\bar{\epsilon}}), \end{aligned} \quad (3.19)$$

which shows the smooth dependence of  $P_1(t)$  on the laser frequency  $\omega$  across threshold.

For times  $t \gtrsim T_{\bar{\epsilon}}$  the short-time behavior as described by Eq. (3.16) is modified. This can be seen from Fig. 5 which shows the ionization probability  $P_1(t)$  as a function of time for the same parameters as have been used in Fig. 2(d). Typically we see the exponentially increasing short-time behavior, which reaches a stationary value after a time of the order of  $1/\Gamma$ . For  $t \gtrsim T_{\bar{\epsilon}}$  we observe the contributions due to the return of the gen-

erated wave packet to the inner turning point of its orbit. The rapid oscillations of the ionization signal thereby reflect quantum-mechanical interferences between ionization amplitudes associated with successive returns.

In the long-time limit when many terms contribute

$$\langle P_1(t) \rangle = \frac{1}{2} + (1/\pi) \arctan(2\bar{\epsilon}/\Gamma) + \sum_{m=1}^{\infty} (\Gamma/\pi) (-2\epsilon)^{-1} (2\pi/|\Phi^{(2)}|) \left[ (1/\pi) \frac{\Gamma/2}{(\epsilon - \bar{\epsilon})^2 + (\Gamma/2)^2} \right]_{\epsilon = \epsilon_s(m,t)}. \quad (3.20)$$

Replacing the sum by an integral we obtain for  $t \gg \Gamma^{-3/2}$ ,

$$\langle P_1(t) \rangle = \frac{1}{2} + (1/\pi) \arctan(2\bar{\epsilon}/\Gamma) - \frac{\Gamma^{1/2}}{\pi^2} \left[ \frac{1}{2} [(2\bar{\epsilon}/\Gamma)^2 + 1]^{-1/4} \cos \left[ \frac{\phi - \pi}{2} \right] + [(2\bar{\epsilon}/\Gamma)^2 + 1]^{1/4} \sin \left[ \frac{\phi - \pi}{2} \right] \right] - \frac{1}{3} (t/2\pi)^{-1} \frac{\Gamma}{\pi} \left[ \frac{1}{\pi} \frac{\Gamma/2}{\bar{\epsilon}^2 + (\Gamma/2)^2} \right]^2. \quad (3.21)$$

This shows that  $\langle P_1(t) \rangle$  is monotonically increasing in time and reaches its stationary value according to a power law involving  $t^{-1}$ , which is in agreement with the numerical study in Ref. 2. The behavior of  $\langle P_1(t) \rangle$  as a function of time is shown in Fig. 5 (dashed curve).

#### IV. PHOTON ABSORPTION FROM EXCITED CHANNELS

As has been discussed in detail in Ref. 11 the problem of Rydberg states in laser fields can be formulated as a scattering-type problem where the laser-induced dynamics can be described as a finite-range coupling of Coulomb fragmentation channels, once the asymptotic (elastic) oscillations of the electron in the laser field are removed. This allows the definition of a radiative reaction matrix, which is a smooth function of energy across the Rydberg threshold and for the case of hydrogen in a circularly polarized light has been obtained numerically in Ref. 11 by solving a system of close-coupling equations in a space-translated frame. The essential result of

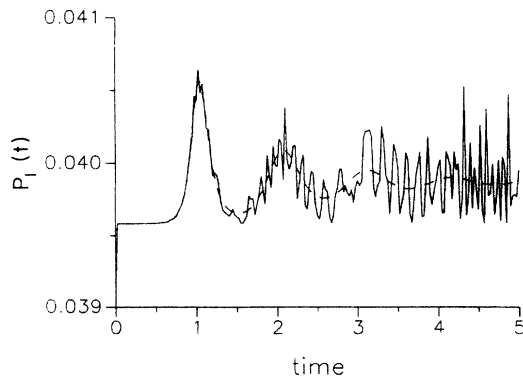


FIG. 5. Ionization probability  $P_1(t)$  as a function of time (in units of  $T_e$ ) for the same parameters as have been used in Fig. 2(d). The dashed curve shows the mean ionization probability.

simultaneously at time  $t$  to the sum in Eq. (3.15) we can define a mean ionization probability in analogy to the mean initial-state probability of Sec. II. Neglecting for simplicity autoionization we thus find with the help of Eq. (3.15)

this work is that the laser-induced couplings between channels can be treated in analogy to configuration mixing of Rydberg series.

Let us now consider a variant of the excitation scheme already studied in Sec. II [Fig. 1(a)], where instead of an autoionizing decay of the Rydberg states the electron can be ionized to a second channel from Rydberg states of channel 1 by absorbing a further laser photon [see Fig. 1(c)]. As mentioned above the coupling of these two channels can be described by a radiative reaction matrix  $\mathcal{R}(\epsilon)$ . In lowest-order Born approximation, which is valid for light intensities  $I$  such that the elastic oscillation amplitude  $\alpha_0$  of the electron in the laser field is small, i.e.,  $\alpha_0 = \sqrt{I} \omega^{-2} \ll 1$  (the a.u. of intensity is  $I_0 = 1.41 \times 10^{17}$  W/cm<sup>2</sup>), the radiative reaction matrix is given by<sup>11</sup>

$$\mathcal{R}(\epsilon) = \begin{bmatrix} 0 & \xi \\ \xi & 0 \end{bmatrix} \quad (\epsilon > 0) \quad (4.1)$$

with the dipole matrix element

$$\xi = \pi \langle \epsilon 1 | d^* \mathcal{G}^* | \epsilon + \omega 2 \rangle \quad (4.2)$$

between the energy normalized Coulomb eigenstates  $|\epsilon j\rangle$  of channel  $j=1,2$  and energy  $\epsilon$ . The corresponding unitary scattering matrix is given by

$$\begin{aligned} \chi &= [1 + i\mathcal{R}(\epsilon)][1 - i\mathcal{R}(\epsilon)]^{-1} \\ &= \begin{bmatrix} (1 - \xi^2)/(1 + \xi^2) & 2i\xi/(1 + \xi^2) \\ 2i\xi/(1 + \xi^2) & (1 - \xi^2)/(1 + \xi^2) \end{bmatrix} \\ & \quad (\epsilon > 0). \quad (4.3) \end{aligned}$$

Comparing Eqs. (4.3) and (3.4) we notice the correspondence with the  $\chi$  matrix of the autoionization problem already studied in Sec. III ( $\alpha = \delta = 0, \tau = \xi^2 \ll 1$ ). The finite range of the radiative coupling implies that the channel-coupling parameter  $\xi$  is approximately energy independent across threshold and that all methods developed in Appendix A for determining below-threshold quantities still apply. Using these methods we

find that below threshold the scattering matrix exhibits poles at the complex energies

$$\varepsilon_n = -\frac{1}{2}(n - i\xi^2/\pi)^2 \approx -1/2n^2 - i\gamma_n/2. \quad (4.4)$$

The imaginary part

$$\gamma_n = 2\pi n^{-3} |\langle \varepsilon 1 | d^* \mathcal{E}^* | \varepsilon + \omega 2 \rangle|^2$$

is the ionization rate of the bound state  $|n\rangle$  in agreement with Fermi's golden rule. [A consistent perturbative evaluation of the above-threshold scattering matrix  $\chi$  up to second order in the coupling parameter  $\alpha_0$  would result in phase shifts of the excited channels proportional to the laser intensity, which are analogous to  $\alpha$  and  $\delta$  in the autoionization problem of Sec. III. In Eq. (4.4) the phase shift associated with channel 1 would give rise to an intensity-dependent energy shift (quadratic Stark shift).]

Using the above threshold scattering matrix of Eq. (4.3) and the results of Appendix A we are able to obtain the initial-state amplitude as a function of time. Due to the formal correspondence with the autoionization problem the effects due to radiative interchannel coupling are the same as the ones already studied in Sec. III.

## V. CONCLUSIONS

We have studied laser excitation of a Rydberg series from a low-lying atomic state. In our theory we have treated radiative excitation and configuration interaction in a unified way using the fact that both act within a reaction zone small in comparison with the extent of the excited Rydberg states. Effects due to configuration interaction or ionization from the excited Rydberg states, which all take place inside the reaction zone, have been taken into account. We have derived analytical expressions for transition amplitudes as a function of time, frequency, and intensity in a *dressed state representation* and by using a *multiple scattering expansion*. In particular, the multiple scattering expansion, which is convenient for describing excitation close to threshold, leads to the simple physical picture of a (radial) electronic wave packet which is generated by the laser-excitation process inside the reaction zone. Every time this wave packet returns to the inner turning point of its orbit (which is located in the reaction zone) it is deexcited back to the initial atomic state which corresponds to stimulated recombination of the disintegrated electron-ion complex. This manifests itself in oscillations of the initial-state probability as a function of time with the period of the classical orbit time. The spreading of the excited wave packet leads to a broadening of the stimulated recombination peaks.

## APPENDIX A

In this appendix we consider the radiative coupling between one low-lying bound state (bound channel) and an arbitrary number of excited Coulomb-fragmentation (free) channels. Within the framework of a QDT treatment we calculate the self-energy of the bound state and

the excitation amplitudes into the free channels. The generalization to more bound channels is straightforward.

We start from the generalization of Eqs. (3.2) and (3.3) to  $N$  free channels, which is given in compact matrix notation by

$$(\varepsilon - \varepsilon_g - \omega) a_g(\varepsilon - \omega) + \int_0^\infty d\rho D^\dagger(\rho) \cdot F(\rho, \varepsilon) = i, \quad (A1)$$

$$(\varepsilon - \mathcal{H}) \cdot F(\rho, \varepsilon) + D(\rho) a_g(\varepsilon - \omega) = 0 [\text{Im}(\varepsilon) = +0]. \quad (A2)$$

The  $N$  components of the column vectors  $F(\rho, \varepsilon)$  and  $D(\rho)$  are the radial channel functions  $F^{(i)}(\rho, \varepsilon)$  and the dipole matrix elements  $D_i(\rho)$  with  $i = 1, \dots, N$ . The radial Hamiltonian  $\mathcal{H}$  characterizes the interchannel coupling between the  $N$  free channels and includes the threshold energies  $\varepsilon_i^{(i)}$  of channels  $i = 1, \dots, N$ . If  $\varepsilon_i = \varepsilon - \varepsilon_i^{(i)} > 0$  then channel  $i$  is open, otherwise it is closed.

If all  $N$  channels are open the physical solution of Eq. (A2), which is bounded for all  $\rho \in [0, \infty)$ , is given by

$$F(\rho, \varepsilon) = F_1(\rho, \varepsilon) = -(\varepsilon - \mathcal{H})^{-1} \cdot D(\rho) a_g(\varepsilon - \omega) \\ \sim \phi^{(+)}(\rho, \varepsilon) \cdot \mathcal{B}(\varepsilon) / 2 \quad (\rho \rightarrow \infty). \quad (A3)$$

$\phi^{(\pm)}(\rho, \varepsilon)$  is the diagonal  $N \times N$  matrix of energy-normalized outgoing (+) [incoming (-)] Coulomb functions as defined in Ref. 8. The column vector  $\mathcal{B}(\varepsilon)$  is determined by Eq. (A2), from which we obtain

$$\frac{1}{2} \left[ \mathcal{F}^{(-)\dagger}(\rho, \varepsilon) \cdot \left[ \frac{d}{d\rho} F(\rho, \varepsilon) \right] \right. \\ \left. - \left[ \frac{d}{d\rho} \mathcal{F}^{(-)}(\rho, \varepsilon) \right]^\dagger \cdot F(\rho, \varepsilon) \right]_{\rho \rightarrow \infty} \\ = - \int_0^\infty d\rho \mathcal{F}^{(-)\dagger}(\rho, \varepsilon) \cdot D(\rho) a_g(\varepsilon - \omega) \\ = - \mathcal{D}_\varepsilon^{(-)} a_g(\varepsilon - \omega). \quad (A4)$$

$\mathcal{F}^{(\pm)}(\rho, \varepsilon)$  is the  $N \times N$  matrix of linear-independent energy-normalized solutions of the homogeneous part of Eq. (A2), which asymptotically behave as

$$\mathcal{F}^{(-)}(\rho, \varepsilon) \sim \frac{1}{2} [\phi^{(+)}(\rho, \varepsilon) - \phi^{(-)}(\rho, \varepsilon) \cdot \chi^*] \quad (\rho \rightarrow \infty) \\ \mathcal{F}^{(+)}(\rho, \varepsilon) \sim \frac{1}{2} [\phi^{(-)}(\rho, \varepsilon) - \phi^{(+)}(\rho, \varepsilon) \cdot \chi] \quad (\rho \rightarrow \infty). \quad (A5)$$

The first index of  $\mathcal{F}^{(\pm)}(\rho, \varepsilon)$  labels the channel components and the second one identifies a particular solution.  $\chi$  is a smooth function of energy across threshold. The components  $\mathcal{D}_{ei}^{(-)}$  of the column vector  $\mathcal{D}_\varepsilon^{(-)}$  are photoionization dipole matrix elements. Inserting Eq. (A3) into Eq. (A4) and using the relation  $\mathcal{W}(\phi_i^{(+)}(\rho, \varepsilon), \phi_i^{(-)}(\rho, \varepsilon)) = -4i/\pi$  for the Wronskian we find

$$\mathcal{B}(\varepsilon) = 2i\pi \mathcal{D}_\varepsilon^{(-)} a_g(\varepsilon - \omega). \quad (A6)$$

Using Eqs. (A3), (A1), and (2.4) we find for the self-energy above threshold

$$\Sigma(\varepsilon) = \delta\omega - i\Gamma/2 \quad [\text{Im}(\varepsilon) = +0] \quad (A7)$$

with the quadratic Stark shift  $\delta\omega$  and the total ionization

rate  $\Gamma = 2\pi\mathcal{D}_\varepsilon^{(-)\dagger}\cdot\mathcal{D}_\varepsilon^{(-)}$ .

In order to determine  $\Sigma(\varepsilon)$  for channels  $i=1, \dots, N_c < N$  closed we have to find a solution of Eq. (A2), which is bounded for all  $\rho \in [0, \infty)$ . For this purpose we use the general solution of Eq. (A2)

$$F(\rho, \varepsilon) = \mathcal{F}^{(+)}(\rho, \varepsilon) \cdot \mathcal{A}(\varepsilon) + F_1(\rho, \varepsilon) \quad [\text{Im}(\varepsilon) = +0] \quad (\text{A8})$$

and determine the column vector  $\mathcal{A}(\varepsilon)$  by the requirement that  $F(\rho, \varepsilon)$  has to be finite for  $\rho \rightarrow \infty$ . Using the asymptotic expansions of  $\phi^{(\pm)}(\rho, \varepsilon)$  (Ref. 8) we find for the open  $[\mathcal{A}_o(\varepsilon)]$  and closed  $[\mathcal{A}_c(\varepsilon)]$  channel components

$$\begin{aligned} \mathcal{A}_o(\varepsilon) &= 0 \quad (i = N_c + 1, \dots, N), \\ \mathcal{A}_c(\varepsilon) &= (\chi_{cc} - e^{-2i\pi\nu c})^{-1} \cdot \mathcal{B}_c(\varepsilon) \quad (i = 1, \dots, N_c). \end{aligned} \quad (\text{A9})$$

$\chi_{cc}$  is the scattering matrix in the closed-channel subspace and  $e^{2i\pi\nu c}$  is a diagonal  $N_c \times N_c$  matrix containing the effective quantum numbers  $\nu_i(\varepsilon) = [-2(\varepsilon - \varepsilon_f^{(i)})]^{-1/2}$ ,  $i = 1, \dots, N_c$ . Inserting Eq. (A8) into Eq. (A1) we obtain the self-energy

$$\Sigma(\varepsilon) = \delta\omega - i\Gamma/2 - 2i\pi\mathcal{D}_{\varepsilon c}^{(-)T} \cdot (\chi_{cc} - e^{-2i\pi\nu c})^{-1} \cdot \mathcal{D}_{\varepsilon c}^{(-)}. \quad (\text{A10})$$

The excitation amplitudes of the excited channels can be derived from Eq. (A2) and the relation

$$(\varepsilon' - \mathcal{H}) \cdot \mathcal{F}^{(-)}(\rho, \varepsilon') = 0, \quad \text{Im}(\varepsilon') = 0$$

which imply

$$(\varepsilon - \varepsilon') \langle \mathcal{F}^{(-)}(\varepsilon') | F(\varepsilon) \rangle = -\mathcal{D}_{\varepsilon'}^{(-)} a_g(\varepsilon - \omega) \quad [\text{Im}(\varepsilon) = +0]. \quad (\text{A11})$$

The excitation amplitude of channel  $i$ ,  $a_{\varepsilon'}^{(i)}(\varepsilon)$ , is therefore given by

$$\begin{aligned} a_{\varepsilon'}^{(i)}(\varepsilon) &= \langle \mathcal{F}^{(-)}(\varepsilon') | F(\varepsilon) \rangle_i \\ &= -\mathcal{D}_{\varepsilon'}^{(-)} (\varepsilon - \varepsilon')^{-1} a_g(\varepsilon - \omega). \end{aligned} \quad (\text{A12})$$

## APPENDIX B

In this appendix we derive Eqs. (2.19) and (3.12) for the case of one bound and  $N$  free channels. Inserting the self-energy of Eq. (A10) into Eq. (A1) we find for channels  $i = 1, \dots, N_c$  (closed),

$$\begin{aligned} a_g(\varepsilon - \omega) &= i[\varepsilon - \bar{\varepsilon} + i\Gamma/2 + 2i\pi\mathcal{D}_{\varepsilon c}^{(-)T} \cdot (\chi_{cc} - e^{-2i\pi\nu c})^{-1} \cdot \mathcal{D}_{\varepsilon c}^{(-)}]^{-1} \\ &= i(\varepsilon - \bar{\varepsilon} + i\Gamma/2)^{-1} + 2\pi(\varepsilon - \bar{\varepsilon} + i\Gamma/2)^{-1} \mathcal{D}_{\varepsilon c}^{(-)T} \cdot (\chi_{cc} - e^{-2i\pi\nu c})^{-1} \\ &\quad \cdot \mathcal{D}_{\varepsilon c}^{(-)} \cdot ((\varepsilon - \bar{\varepsilon} + i\Gamma/2) \{ (\chi_{cc} - e^{-2i\pi\nu c})^{-1} \cdot \mathcal{D}_{\varepsilon c}^{(-)} \}^{-1} \\ &\quad + 2i\pi(\varepsilon - \bar{\varepsilon} + i\Gamma/2)^{-1} \mathcal{D}_{\varepsilon c}^{(-)T} \} \cdot (\chi_{cc} - e^{-2i\pi\nu c})^{-1} \cdot \mathcal{D}_{\varepsilon c}^{(-)})^{-1} \\ &= i(\varepsilon - \bar{\varepsilon} + i\Gamma/2)^{-1} + 2\pi [ -(\varepsilon - \bar{\varepsilon} + i\Gamma/2)^{-1} \mathcal{D}_{\varepsilon c}^{(-)T} ] \cdot \{ e^{2i\pi\nu c} \cdot [1 - \tilde{\chi}_{cc}(\varepsilon) \cdot e^{2i\pi\nu c}]^{-1} \} \cdot [\mathcal{D}_{\varepsilon c}^{(-)} (\varepsilon - \bar{\varepsilon} + i\Gamma/2)^{-1}]. \end{aligned} \quad (\text{B1})$$

Expanding the term in curly brackets after the last equality sign in Eq. (B1) into a geometric series we obtain

$$a_g(\varepsilon - \omega) = i(\varepsilon - \bar{\varepsilon} + i\Gamma/2)^{-1} + 2\pi [i(\varepsilon - \bar{\varepsilon} + i\Gamma/2)^{-1} \mathcal{D}_{\varepsilon c}^{(-)T}] \cdot e^{2i\pi\nu c} \cdot \sum_{m=1}^{\infty} [\tilde{\chi}_{cc}(\varepsilon) e^{2i\pi\nu c}]^{m-1} \cdot [\mathcal{D}_{\varepsilon c}^{(-)} i(\varepsilon - \bar{\varepsilon} + i\Gamma/2)^{-1}] \quad (\text{B2})$$

with

$$\tilde{\chi}(\varepsilon) = \chi + 2i\pi\mathcal{D}_\varepsilon^{(-)} (\varepsilon - \bar{\varepsilon} + i\Gamma/2)^{-1} \cdot \mathcal{D}_\varepsilon^{(-)T}. \quad (\text{B3})$$

The first term of Eq. (B3) characterizes the finite-range

coupling between the  $N$  free channels whereas the second term is due to the radiative coupling to the bound channel.

<sup>1</sup>A. I. Andryushin, A. E. Kazakov, and M. V. Fedorov, Zh. Eksp. Teor. Fiz. **76**, 1907 (1979) [Sov. Phys.—JETP **49**, 966 (1979)].

<sup>2</sup>J. Javanainen, Opt. Commun. **46**, 175 (1983).

<sup>3</sup>C. Cohen-Tannoudji, B. Diu, and F. Laloe, Quantum Mechanics (Wiley, New York, 1977).

<sup>4</sup>E. Kyrölä, J. Phys. B **19**, 1437 (1986) and references therein.

<sup>5</sup>For the coupling between a discrete and a set of evenly spaced quasicontinuum states see, e.g., P. W. Milonni, J. R. Ack-

erhalt, N. W. Galbraith, and Mei-Li Shih, Phys. Rev. A **28**, 32 (1983); E. Kyrölä and J. H. Eberly, J. Chem. Phys. **82**, 1841 (1985).

<sup>6</sup>P. Zoller, G. Alber, and H. Ritsch in *Proceedings of the Fourth International Symposium on Quantum Optics, Hamilton, New Zealand* (Springer, Berlin, 1986).

<sup>7</sup>For the breakdown of the pole approximation in photodetachment see, e.g., K. Rzazewski, M. Lewenstein, and J. H. Eberly, J. Phys. B **15**, L661 (1982); J. Javanainen, *ibid.* **16**, 1343

- (1983); A. I. Andryushin, M. V. Fedorov, and A. E. Kazakov, *ibid.* **17**, 3469 (1984); S. L. Haan and J. Cooper, *ibid.* **17**, 3481 (1984).
- <sup>8</sup>M. J. Seaton, *Rep. Prog. Phys.* **46**, 167 (1983).
- <sup>9</sup>R. H. Bell and M. J. Seaton, *J. Phys. B* **18**, 1589 (1985).
- <sup>10</sup>U. Fano and A. R. P. Rau, *Atomic Collision and Spectra* (Academic, New York, 1986).
- <sup>11</sup>A. Giusti-Suzor and P. Zoller, *Phys. Rev. A* **36**, 5178 (1987).
- <sup>12</sup>The multiple scattering expansion in semiclassical scattering theory is discussed, e.g., in W. H. Miller, *Adv. Chem. Phys.* **30**, 77 (1975).
- <sup>13</sup>A similar expression based on model assumptions about the energy dependence of the involved dipole matrix elements has been used in Ref. 2 as the starting point of a numerical analysis.
- <sup>14</sup>U. Fano, *Phys. Rev.* **124**, 1866 (1961).
- <sup>15</sup>Autoionizinglike resonances are discussed, e.g., by L. Armstrong, Jr., B. L. Beers, and S. Feneuille, *Phys. Rev. A* **12**, 1903 (1975); Y. I. Heller and A. K. Popov, *Opt. Commun.* **18**, 449 (1976); P. E. Coleman, P. L. Knight, and K. Burnett, *ibid.* **42**, 171 (1982).
- <sup>16</sup>L. Dimou and F. H. M. Faisal in *Photons and Continuum States of Atoms and Molecules*, edited by N. K. Rahman, C. Guidotti, and M. Allegrini (Springer, Berlin, 1986).
- <sup>17</sup>A result similar in structure but without giving analytical expressions for the residuum contributions due to the dressed states has been obtained in Ref. 1.
- <sup>18</sup>*Handbook of Mathematical Functions*, Natl. Bur. Stand. Appl. Math. Ser. No. 55, edited by M. Abramowitz and I. Stegun (U.S. GPO, Washington, D.C., 1964).
- <sup>19</sup>H. Goldstein, *Classical Mechanics*, 2nd ed. (Addison-Wesley, Reading, Mass., 1980).
- <sup>20</sup>J. N. Connors in *Semiclassical Methods in Molecular Scattering and Spectroscopy*, edited by M. S. Child (Reidel, Dordrecht, 1980).
- <sup>21</sup>A. Giusti-Suzor and H. Lefebvre-Brion, *Phys. Rev. A* **30**, 3057 (1984).
- <sup>22</sup>P. Lambropoulos and P. Zoller in *Multiphonon Ionization of Atoms*, edited by S. L. Chin and P. Lambropoulos (Academic, New York, 1986).